



# Current progress and future perspectives for organic/inorganic perovskite solar cells

Pablo P. Boix<sup>1</sup>, Kazuteru Nonomura<sup>1</sup>, Nripan Mathews<sup>1,2,3,\*</sup> and Subodh G. Mhaisalkar<sup>1,2,\*</sup>

<sup>1</sup>Energy Research Institute @NTU (ERI@N), Research Techno Plaza, X-Frontier Block, Level 5, 50 Nanyang Drive, Singapore 637553, Singapore

<sup>2</sup>School of Materials Science and Engineering, Nanyang Technological University, Nanyang Avenue, Singapore 639798, Singapore

<sup>3</sup>Singapore-Berkeley Research Initiative for Sustainable Energy, 1 Create Way, Singapore 138602, Singapore

The recent emergence of efficient solar cells based on organic/inorganic lead halide perovskite absorbers promises to transform the fields of dye-sensitized, organic, and thin film solar cells. Solution processed photovoltaics incorporating perovskite absorbers have achieved efficiencies of 15% [1] in solid-state device configurations, superseding liquid dye sensitized solar cell (DSC), evaporated and tandem organic solar cells, as well as various thin film photovoltaics; thus establishing perovskite solar cells as a robust candidate for commercialization. Since the first reports in late 2012, interest has soared in the innovative device structures as well as new materials, promising further improvements. However, identifying the basic working mechanisms, which are still being debated, will be crucial to design the optimum device configuration and maximize solar cell efficiencies. Here we distill the current state-of-the-art and highlight the guidelines to ascertain the scientific challenges as well as the requisites to make this technology market-viable.

## Introduction

Achieving cost effective, easily processable, efficient and versatile solar cells has always been a challenge for the scientific community [2]. An attractive candidate fulfilling these requirements is the sensitized solar cell architecture. Since the development of the dye sensitized solar cell (DSC) [3] which is the ultimate expression of this configuration, power conversion efficiencies have reached 12.3% [4]. The possibility of replacing volatile liquid electrolyte with a solid hole transport material (HTM) has been pursued [5], but low efficiencies ( $\eta < 10\%$  [6,7]) have been a drawback for the commercialization of this technology. In order to improve the efficiency of the solid state DSC (ssDSC), different approaches have been explored. This includes dye design for extending the absorption range towards the near infrared regime as well as increasing electron injection and hole regeneration. However the obtained efficiency remains low, since the poor optical extinction coefficient requires a thick

mesoporous film to absorb the light, increasing hole transport resistance and recombination.

Quantum dot solar cells (QDSC) utilize semiconductor nanocrystals as light absorbers [8]. Their large intrinsic dipole moment and tunability of the bandgap by size control and shape provide an excellent tool for nanoscale design of light absorber materials for sensitized solar cells. In solid state configuration remarkable efficiencies higher than 8% have been reported for innovative devices structures, where PbS absorber acts as HTM [9]. Similarly, extremely thin absorber (ETA) solar cells use a thin layer of inorganic absorber to sensitize a mesoporous semiconductor.  $\text{Sb}_2\text{S}_3$  has achieved excellent solid state efficiencies in this configuration due to its low bandgap and high extinction coefficient. Nevertheless problems such as high recombination have not been overcome yet, limiting its maximum efficiency to 6.3% when combined with the appropriate polymer and fullerene derivative [10]. Other inorganic materials have also been employed as sensitizers for  $\text{TiO}_2$  including  $\text{CuInS}_2$  (CIS), achieving efficiencies of 5% [11].

\*Corresponding authors: Mathews, N. (Nripan@ntu.edu.sg), Mhaisalkar, S.G. (Subodh@ntu.edu.sg)

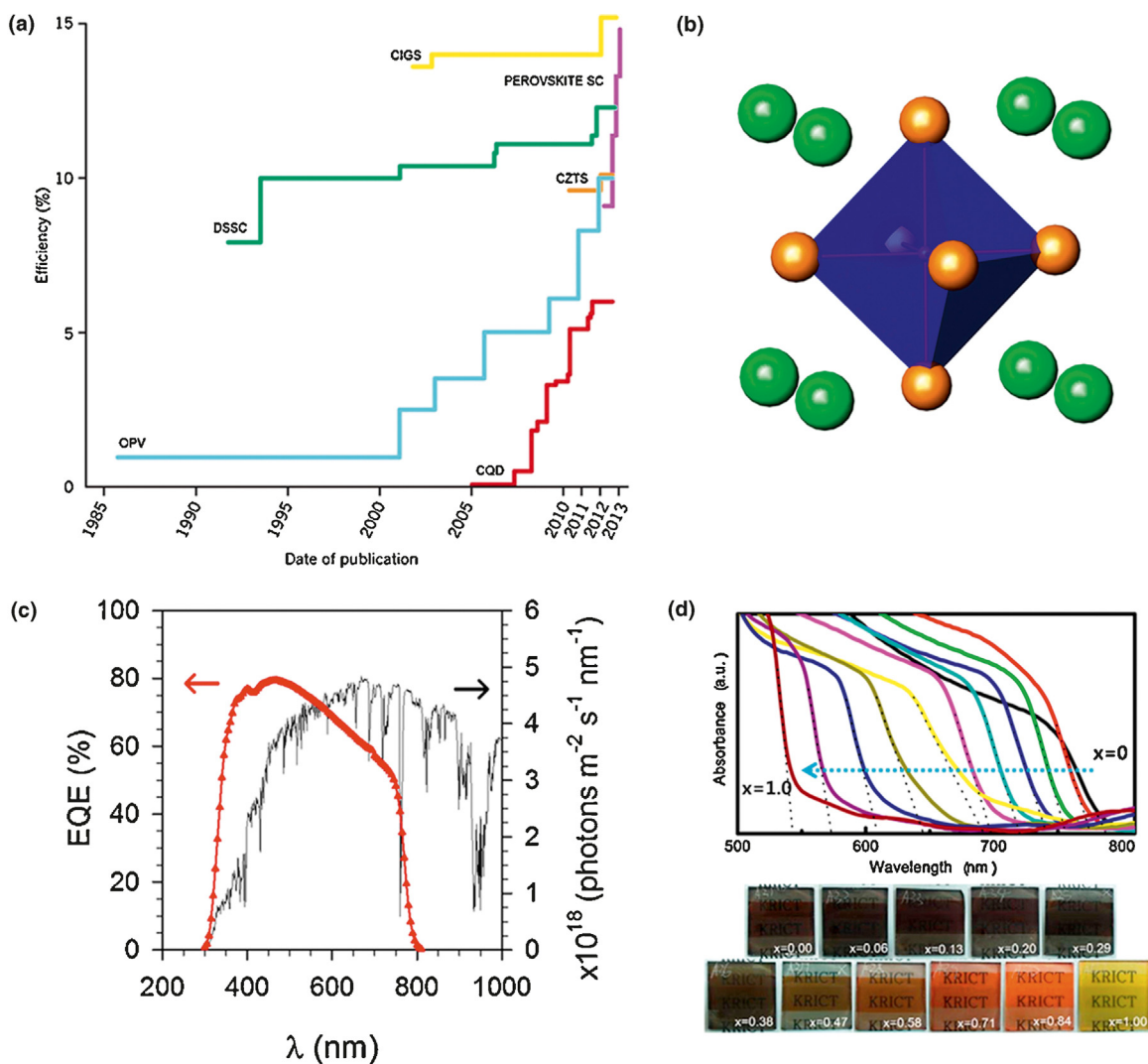


FIGURE 1

(a) Efficiency charts for solution processed solar cells. Data adapted from Ref. [2], (b)  $\text{CH}_3\text{NH}_3\text{PbI}_3$  perovskite structure, (c) external quantum efficiency measured for a  $\text{CH}_3\text{NH}_3\text{PbI}_3$  perovskite solar cell and AM1.5 g solar spectra and (d) absorption measured for different  $\text{TiO}_2/\text{CH}_3\text{NH}_3\text{PbI}_{3-x}\text{Br}_x$  films. Reprinted from Ref. [36].

Since late 2012, organic/inorganic halides with the perovskite structure have strongly attracted the attention of the photovoltaic community when efficiencies close to 10% were first achieved in solid state cells [12,13]. The excellent properties and the innovative device possibilities in perovskite-structured organometal halides has resulted in a frenzied increase of publications reporting high efficiencies [14,15], see Fig. 1a. Recently 15% efficient solar cells were reported with  $\text{CH}_3\text{NH}_3\text{PbI}_3$  [1] target efficiencies of 20% identified as a feasible goal [16]. It is therefore pertinent to evaluate the potential and analyze the prospects of this exciting technology that have galvanized the photovoltaic research community.

Here we summarize the photovoltaic studies with organometal halide perovskite compounds and propose avenues for further development. The optical and electrical characteristics of these halides are reviewed and compared to other sensitizers. The wide variety of device architectures employed so far, are evaluated. Since different architectures have diverse principles determining their performance, these insights into the working mechanisms allow the determination of the optimum approach. At the end,

future perspectives with a particular focus in the improvement of efficiency, stability commercialization prospects are discussed.

### Organic/inorganic metal halides as light absorbers

Although these class of materials have been widely studied for decades [17,18], only recently have they been introduced in solar cells. The first reports based on hybrid organic/inorganic halides  $\text{CH}_3\text{NH}_3\text{PbI}_3$  and  $\text{CH}_3\text{NH}_3\text{PbBr}_3$ , published in 2009, achieved 3.8% efficiencies in a liquid electrolyte configuration [19] where the absorber was regarded as a QDs deposited on  $\text{TiO}_2$ . The efficiency was further improved to 6.5% [20], but the short stability of the devices caused due to dissolution of the halides in the electrolyte, appeared to be an enormous drawback. The breakthrough occurred in late 2012 with the introduction of solid state hole transporting layers within the solar cell. This resulted in stable efficiencies close to 10% [12,21], establishing these materials as robust candidates for efficient solar cells. These reports of high efficiency coupled with the materials' excellent optical, electrical and mechanical properties [22–28] along with solution

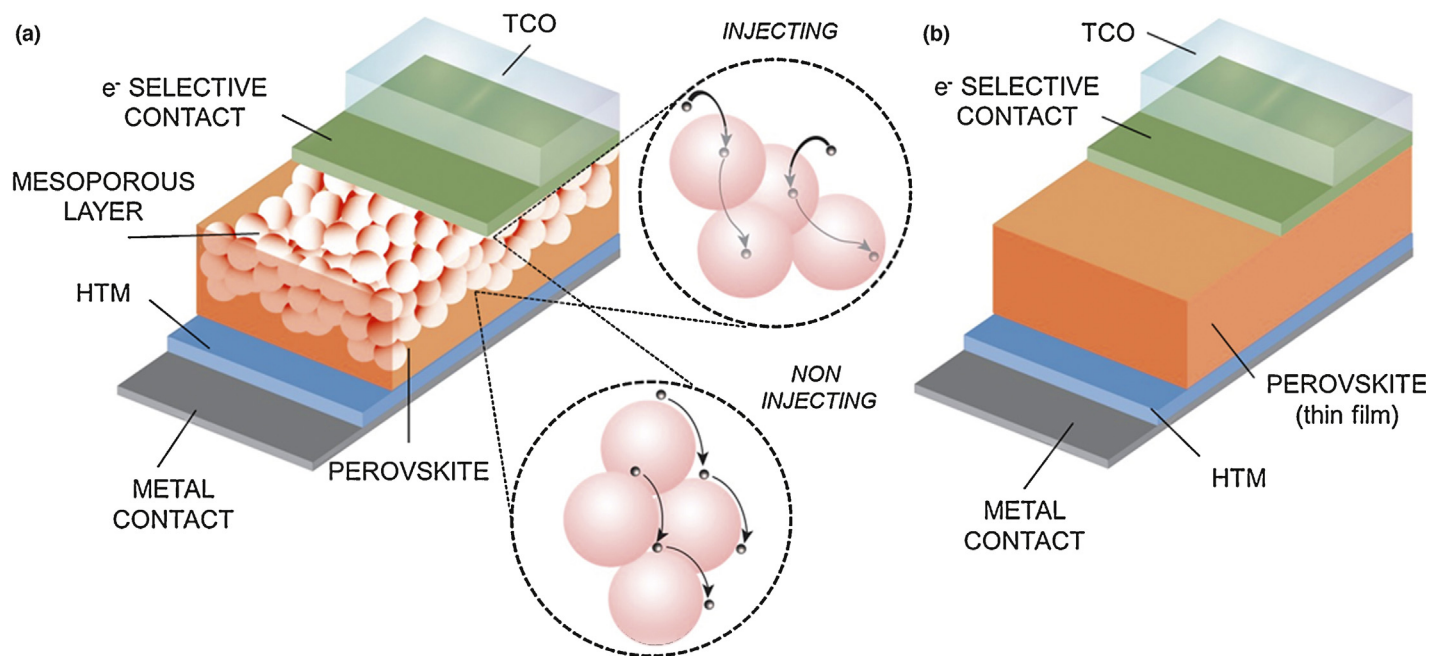


FIGURE 2

Devices structure for (a) mesoporous perovskite solar cell structure where no HTM interpenetration is required. In the inset the electron charge transport processes for injecting and non-injecting mesoporous materials are represented and (b) structure of a thin film-like perovskite solar cell.

processability have triggered rapid and continuous improvements in their efficiencies [14,15]. Furthermore, other perovskite structured materials such as  $\text{CsSnI}_3$  was effectively demonstrated as HTM and absorber in ssDSC, where a combination with N719 dye yielded efficiencies of over 10% [7].

Organic/inorganic perovskites are hybrid layered materials typically with an  $\text{AMX}_3$  structure, with A being a large cation, M a smaller metal cation and X an anion from the halide series. They form an octahedral structure of  $\text{MX}_6$ , which forms a three dimensional structure connected at the corners [29–31] as shown in Fig. 1b. The component A fills the coordinated space between the octahedrals that form in these three-dimensional structures. The size of the cation A is an important aspect for the formation of a closed packed perovskite structure, since this cation A must fit into the space composed of the four adjacent octahedra which are connected together through shared corners [32]. In these organic/inorganic halides, the organic cations are small and are typically restricted to methylammonium, ethylammonium and formamidinium. The integration of larger molecules with terminal cationic groups within the inorganic framework have also been demonstrated in some cases [24,33]. The metal cations are typically divalent metal ions such as  $\text{Pb}^{2+}$ ,  $\text{Sn}^{2+}$  and  $\text{Ge}^{2+}$  while the halide anions are  $\text{I}^-$ ,  $\text{Cl}^-$  and  $\text{Br}^-$ . The optical absorption as well as photoluminescence is related to the metal halide employed, with the iodides resulting in smaller bandgaps and light emission at longer wavelengths while the bromides display higher bandgap and luminescence at shorter wavelengths [34–36]. Interestingly, a perovskite structure which incorporates two halides (e.g. iodide and bromide) allows for the continuous tuning of the bandgap (Fig. 1d) [19,37].

The best solar cells have been obtained from  $\text{CH}_3\text{NH}_3\text{PbI}_3$  which has a bandgap of 1.55 eV, close to the optimum one for

photovoltaic performance ( $\sim 1.4$  eV). This coupled with the good extinction coefficient (one order of magnitude higher than standard dyes [20]) enables excellent external quantum efficiency spectra (EQE) in the solar cells [12,38] until 800 nm, harvesting the photons in the visible range of the solar spectra and part of the near-infrared (see Fig. 1c). Remarkably, when  $\text{CH}_3\text{NH}_3\text{PbI}_3$  is heated above 55–60 °C it undergoes a phase transition from tetragonal to cubic [31], which is expected to narrow the bandgap.

### Solar cell device architectures

The huge interest of  $\text{CH}_3\text{NH}_3\text{PbI}_3$  perovskite does not only lie in the high efficiencies but also in the novel configurations made possible by the singular characteristics of the material.

Metal-halide based devices with structure similar to the classical ssDSC [12] were fabricated with the organic/inorganic halide being deposited in a nanostructured  $\text{TiO}_2$  layer by a single step spin-coating method (device structure in Fig. 2a) and spiro-OMeTAD (2,2',7,7'-tetrakis-(N,N-di-p-methoxyphenylamine)9,9'-spirobifluorene) HTM deposited on top. In this report optical measurements show charge injection from the perovskite into both  $\text{TiO}_2$  (electrons) and HTM (holes), but the latter is the fastest one. Very recently the application of the sequential deposition process (originally developed by Mitzi and coworkers [39]) whereby  $\text{PbI}_2$  is converted into  $\text{CH}_3\text{NH}_3\text{PbI}_3$  within the pores of the  $\text{TiO}_2$  have resulted in record efficiencies ( $\eta = 15.0\%$ , Fig. 3a) [1].

An important alteration of the above architecture was the replacement of the  $\text{TiO}_2$  mesoporous by an insulating  $\text{Al}_2\text{O}_3$  scaffold achieving efficiencies of 10.9% [21]. It is worth to remark that regardless of the mesoporous layer, a compact  $\text{TiO}_2$  layer is still required for both the collection of the generated electrons and hole blocking. Since alumina's conduction band is far higher than

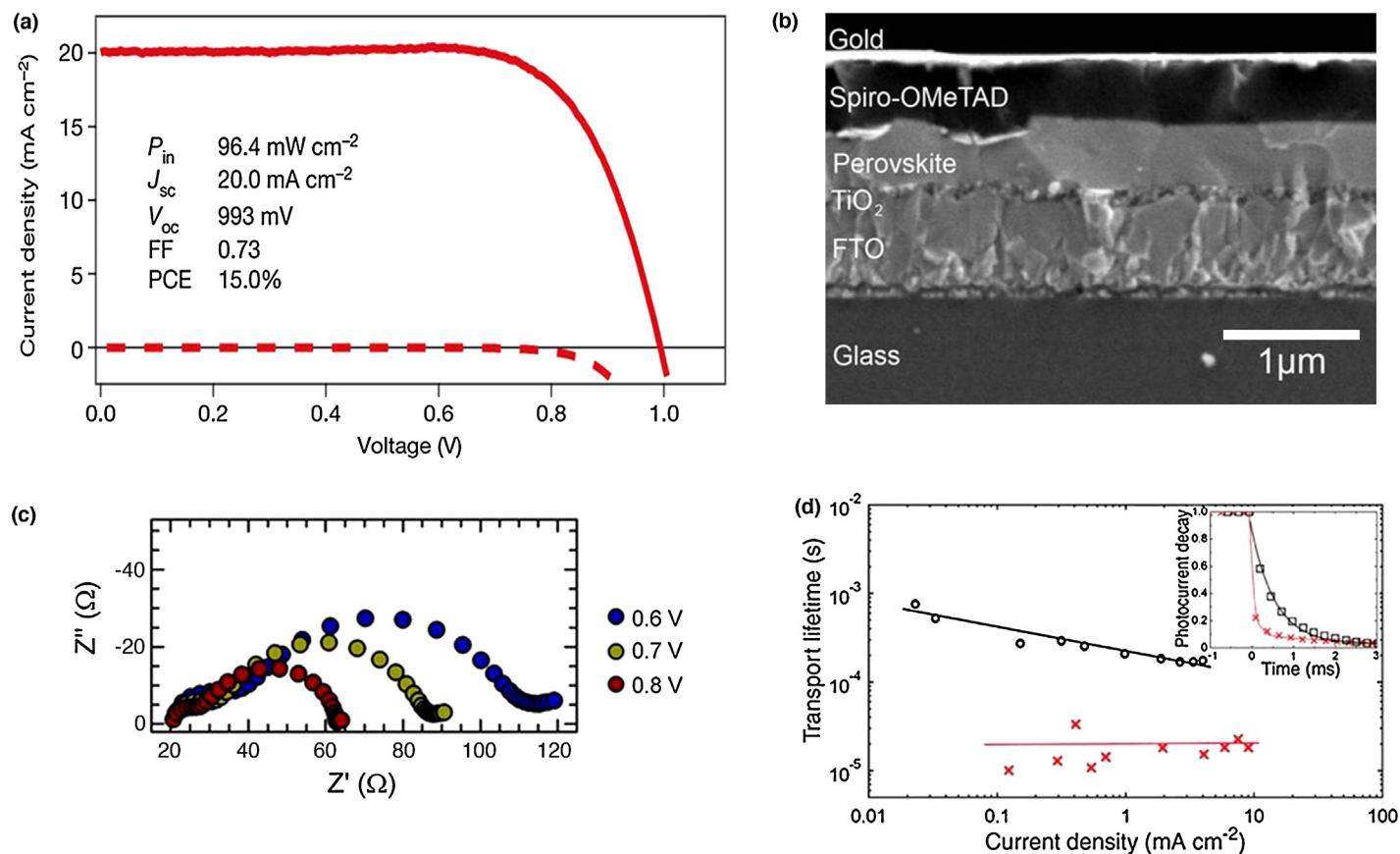


FIGURE 3

(a) Measured current–voltage curve and performance characteristics for the record  $\text{CH}_3\text{NH}_3\text{PbI}_3$  solar cell. Reprinted from Ref. [1], (b) cross section measured for a thin film-like perovskite solar cell with thin scaffold thickness. Reprinted from Ref. [59], (c) impedance spectra measured for a nanorod/ $\text{CH}_3\text{NH}_3\text{PbI}_3$  solar cell. Reprinted from Ref. [38] and (d) charge transport lifetime determined by small perturbation transient photocurrent decay of perovskite sensitized  $\text{TiO}_2$  (circles with black line to aid the eye) and  $\text{Al}_2\text{O}_3$  cells (red crosses with line to aid the eye). Inset shows normalized photocurrent transients for  $\text{TiO}_2$  (black) and  $\text{Al}_2\text{O}_3$  cells (red), reprinted from Ref. [13].

the absorber's LUMO, no electron injection from perovskite takes place. This indicates that the electron transport occurs within  $\text{CH}_3\text{NH}_3\text{PbI}_{3-x}\text{Cl}_x$  perovskite, which is confirmed by photoinduced absorption spectroscopy (PIA) measurements of the  $\text{Al}_2\text{O}_3/\text{CH}_3\text{NH}_3\text{PbI}_{3-x}\text{Cl}_x$  layers [21]. In contrast, PIA measurements of  $\text{CH}_3\text{NH}_3\text{PbI}_{3-x}\text{Cl}_x/\text{spiro-OMeTAD}$  layers indicated that the photogenerated hole was injected into spiro-OMeTAD. This approach avoids the voltage drop associated with the occupation of the  $\text{TiO}_2$  band-tails [40], thus resulting in higher photovoltage, additionally small-perturbation transient photocurrent decay measurements [13] also show faster charge collection in  $\text{Al}_2\text{O}_3$  based devices compared to the  $\text{TiO}_2$  ones (Fig. 3d). Similar results have been obtained with pure  $\text{CH}_3\text{NH}_3\text{PbI}_3$  in combination with non-injecting  $\text{ZrO}_2$  scaffolds [41]. The highest photovoltage reported so far within these class of materials (1.3 V) also employed this configuration, albeit in conjunction with a higher bandgap Br analogue and N,N'-dialkyl perylenediimide HTM [42]. Several other hole transporting materials such as poly-(3-hexylthiophene-2,5-diyl) (P3HT) and poly[N-900-heptadecanyl-2,7-carbazole-alt-5,5-(40,70-di-2-thienyl-20,10,30-benzothiadiazole)] (PCDTBT) have also been tested with interesting results [14,43], however amine based (spiro-OMeTAD, poly-triarylamine PTAA) HTMs outperform energetically equivalent thiophene derivatives indicating a better interface with the perovskite absorber.

Interestingly, it was also reported that  $\text{CH}_3\text{NH}_3\text{PbI}_3$  perovskite functions concurrently as a hole transporting material and light absorber, with 5.5% conversion efficiency attained with a  $\text{TiO}_2/\text{CH}_3\text{NH}_3\text{PbI}_3$  perovskite/Au construction [44]. Obviously, a good coverage of the  $\text{TiO}_2$  film by the  $\text{CH}_3\text{NH}_3\text{PbI}_3$  is needed in this case, resulting in a thin capping layer, this configuration corresponding to Fig. 2a without the HTM layer. Therefore, it is clear that the electrical transport in organic/inorganic metal halides can occur as an ambipolar diffusion of electrons and holes [15]. This is further supported by recent reports where both electron and holes are extracted from a  $\sim 350$  nm thick layer of  $\text{CH}_3\text{NH}_3\text{PbI}_{3-x}\text{Cl}_x$  absorber sandwiched between a compact  $\text{TiO}_2$  film and hole transporting spiro-OMeTAD. Even in the absence of mesoporous films photocurrent densities close to  $15 \text{ mA cm}^{-2}$  were achieved in an approach analogous to the classical thin film architecture represented in Fig. 2b (without scaffold) or even higher with a minimum scaffold holding the perovskite thin film (Fig. 3b). Planar configurations of  $\text{CH}_3\text{NH}_3\text{PbI}_3$  with other contacts as PEDOT:PSS and various fullerene derivatives also displayed photocurrents of more than  $10 \text{ mA cm}^{-2}$  [45]. A recent report [46] has presented a planar heterojunction perovskite solar cell fabricated by vapor deposition which matched the 15% efficiency record of the mesoporous cell. This result confirms the existence of relatively long range electron, hole transport in these class of materials.

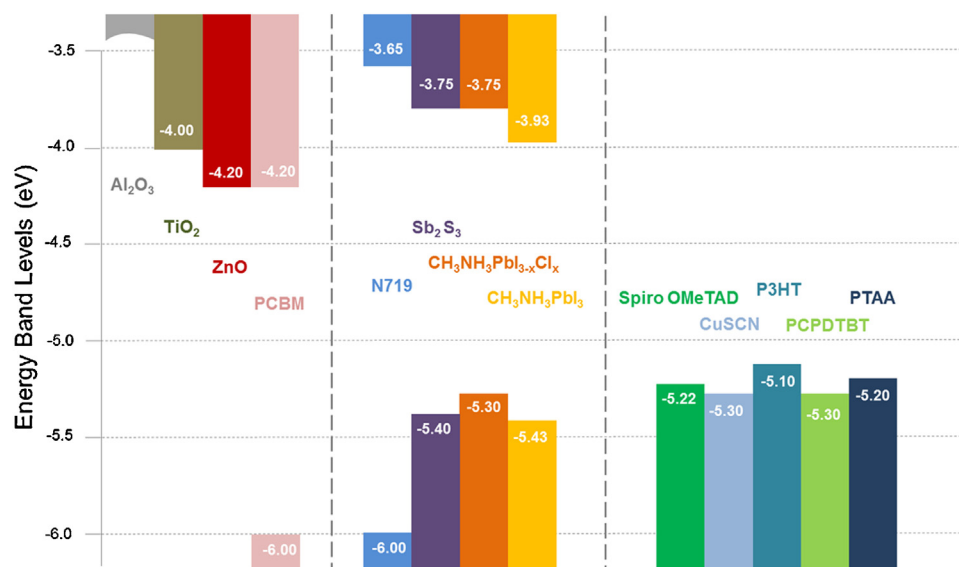


FIGURE 4

Energy levels for different materials acting as electron transporting material (left), absorbers (middle) and hole transporting materials (right) in solar cells.

Due to the wide variety of device architectures and material sets employed in conjunction with the organic/inorganic metal halides, it is important to identify the pertinent mechanisms governing each configuration.

### Photovoltaic operational mechanisms

If we consider the system to be purely analogous to an ssDSC where the absorbed photon is converted into charge by the injection of the electrons and the regeneration of the holes, (inset Fig. 2a) certain features must be considered for understanding the main physical processes governing the cell behaviour.

This model involves a fast injection of carriers from the light absorber into their respective conductive media, with no carrier transport occurring within the absorber itself. In this case, a good distribution of the absorber within the mesoporous layer will ensure maximal interfacial area required to generate the photocurrent. Thus the limitations of this architecture will be analogous to that of the classical ssDSC [47] which have been widely studied. One of the main considerations is the light absorption. As described before, the bandgap of CH<sub>3</sub>NH<sub>3</sub>PbI<sub>3</sub> is close to the optimum for photovoltaic conversion, while the high extinction coefficient of the material ensures a good absorption of the light at low mesoporous film thickness (w.r.t. dye sensitized systems). However, in order to separate the excited state into charge carriers, an energy price has to be paid for both electron and hole injection—directly reflected in the achievable  $V_{OC}$ . When TiO<sub>2</sub> and spiro-OMeTAD are used, the energetic offsets are  $\Delta E \sim 0.07$  eV and  $\Delta E \sim 0.21$  eV for electrons and holes respectively (Figs. 4 and 5a). Under these circumstances, the energetic disorder and defects of the absorber will only have a minor effect in the absorption [40] because both the charge separation and charge transport take place at the interface or outside the absorber material. In contrast, the distribution of energetic states in the transport materials (TiO<sub>2</sub>, HTMs) have an effect in the splitting of the Fermi levels and in the charge transport due to the population of band-tails [40]. This necessitates the development of new nanostructures for electron

separation and conduction such as TiO<sub>2</sub> nanorods [38,48], nanosheets [49] with the objective of improving electron transport and absorber infiltration, as well as exploration of novel HTMs with suitable band alignment and improved hole mobilities [14,43].

In addition to these voltage losses associated with energy level mismatches as well as charge separation, charge recombination can further limit the performance of these devices. In a similar solid state systems such as TiO<sub>2</sub>/Sb<sub>2</sub>S<sub>3</sub>/CuSCN, the bandgap of the absorber (1.65 eV) minus the offset for electron and hole injection indicates 1.30 eV available as a potential difference, however the reported  $V_{OC}$  at 1 sun is only 0.60 V [50]. In comparison, for TiO<sub>2</sub>/CH<sub>3</sub>NH<sub>3</sub>PbI<sub>3</sub>/spiro OMeTAD devices the available potential difference is 1.22 eV while the  $V_{OC}$  achieved is more than 0.9 V [12]. This means that  $\sim 0.7$  V is 'lost' in the Sb<sub>2</sub>S<sub>3</sub> system, while only  $\sim 0.3$  V is lost in the perovskite system. Although this indicates that recombination in perovskite solar cells is much lower than in Sb<sub>2</sub>S<sub>3</sub> devices, carrier lifetime measurements do not seem to support it [43,51]. Additional experiments to compare the CH<sub>3</sub>NH<sub>3</sub>PbI<sub>3</sub> system against other sensitizers under similar device conditions are therefore required.

Another loss mechanisms that affects the performance is manifested when varying the film thickness [12,14]. Thicker films increase the light absorption, but at the same time reduce the EQE and consequently the current, in contrast to classical liquid DSCs. This highlights the importance of studying the recombination losses. Therefore, even considering the encouraging open circuit potentials, the identification of the process controlling the recombination mechanism, its characterization and reduction is critical for improving the efficiency of perovskites solar cells.

Optical measurements as photoinduced absorption spectroscopy (PIA) [52] and transient grating (LF-HD-TG) technique [53]; electrochemical impedance spectroscopy [54] as well as mixed techniques such as transient photovoltage [55] have been used to characterize these losses with good accuracy in sensitized devices. Recently some of these techniques have been applied to

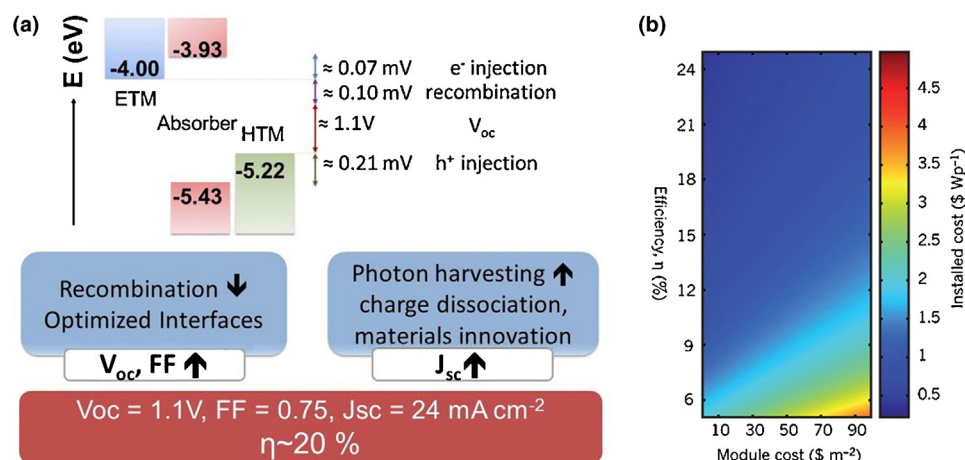


FIGURE 5

(a) Energetics losses and possible avenues for performance improvements in perovskites-based solar cells and (b) cost per Watt peak (Wp) as a function of module cost and module efficiency, as a function of module cost and module efficiency, assuming that balance-of-systems costs can be reduced to US\$100 per square metre. Reprinted from Ref. [2].

organic/inorganic halides solar cells for different absorbers and HTM [43], nevertheless further investigation is needed to understand which recombination process is the dominating one in this new kind of systems.

In contrast to the sensitized solar cell architecture presented above, in solar cells utilizing mesoporous  $\text{Al}_2\text{O}_3$  instead of mesoporous  $\text{TiO}_2$  [15,56], given the energetics of alumina, the injection of electrons from the absorber is not possible (inset, Fig. 2a). As a consequence the extracted electrons must flow within the  $\text{CH}_3\text{NH}_3\text{PbI}_{3-x}\text{Cl}_x$  itself. As seen in previous sections, analogous cases are reported where the absorber materials transport the holes [49]. This configuration thus resembles a thin film solar cell with the scaffold providing roughness to load the absorber layer resulting in efficient light absorption. In order to understand how this thin film configuration works, the nature of the first excited state is a critical factor to consider. If the binding energy of the photo-generated electron-hole pair is low enough (comparable to thermal energy), charge generation can occur within the absorber (like in silicon solar cells [57]). This could be beneficial for the device efficiency since the voltage drop due to the driving force needed to dissociate electron-hole pair can be avoided. Classical studies indicate that the generated electron-hole pair seems to behave as a Mott-Wannier exciton in the  $\text{CH}_3\text{NH}_3\text{PbI}_3$  with low binding energies of 50 meV [34]. This indicates the possibility of charge separation within the absorber itself. This coupled with long charge carrier diffusion lengths can explain the good performance in a thin film configuration [57] (schematically shown in Fig. 2b, device characteristics in Fig. 3c). Electron and hole carrier diffusion lengths can be measured in the perovskite layers by combining them with selective electron or hole acceptors in a bilayer configuration. Primary measurements on such bilayers have shown that electron and hole transport lengths in the perovskite films are balanced and at least 100 nm [58]. These results justify the excellent performance achieved in relatively thick layers (~350 nm) of  $\text{CH}_3\text{NH}_3\text{PbI}_{3-x}\text{Cl}_x$  [15,59], where the device configuration was planar. Increasing the permittivity of the material (leading to low electron-hole binding energy) can enhance the charge generation.

Under this scenario the key physical mechanism of the devices are substantially different. Here the perovskite does not only absorb photons but also transports both electrons and holes, benefiting therefore from ambipolar conduction [15]. Promising conductivities have been reported for perovskite structured materials as  $\text{CsSnI}_3$  [60] and  $\text{CH}_3\text{NH}_3\text{PbI}_3$  [61], but improving the carrier diffusion lengths is a pertinent way of boosting device efficiency. A possible route in this direction could lay in the replacement of the metal cation or the halide anion, as reported for  $\text{CH}_3\text{NH}_3\text{PbI}_3$  perovskite groups where replacing I or Pb modified conductivity [62]. Sn-based perovskites have shown good charge carrier conductivities [63,64], although devices based on this kind of absorbers did not offer photovoltaic performance. While exploring newer classes of perovskite compounds, it is essential that the crystallizing nature of these compounds is not restricted. This is important both for conductivity and charge generation, since the crystallinity determines the distribution of energetic states. In addition to the solution based deposition processes, other techniques such as evaporative deposition may have to be pursued [65]. Perovskites made from different deposition techniques will have to be compared against single crystals (either grown from solution [31] or physical vapor transport [61]) in order to ensure low defect densities and less energetic disorder.

Determining the relative advantage of employing the perovskite purely as a sensitizer (electron-injection into the mesoporous semiconductor) as opposed to a thin film absorber is one of the key issues to be addressed. In the thin film approach the bulk recombination within the perovskite gains prominence, whereas interfacial recombination is dominant in the sensitized architecture. The reduction of the energetic defects that can act as recombination centres or traps in the material is then necessary for efficiency improvement in the thin film configuration. Spatially resolved measurements are a valuable method to investigate the location of charge generation, which in combination with the optoelectrical techniques previously presented will lead to the determination of the applicable model. Impedance spectra (Fig. 2c) can be fitted to extract the chemical capacitance in this kind of devices. Since the chemical capacitance ( $C_\mu$ ) directly

reflects the density of states of the material that is being electrically charged, its determination allows discernment of the perovskite's role. Similar values obtained for  $C_{\mu}$  in  $\text{TiO}_2$  (injecting) and  $\text{ZrO}_2$  (non-injecting) based devices seem to indicate that the conduction through the perovskite could play a prominent role even in the injecting case [66].

Basic questions are still open, and it is an urgent requirement to determine the optimal configuration for these solar cells. Deeper research of this matter can open new pathways to increase efficiency, contingent on a more complete understanding of the working principles of these devices.

### Prospects, efficiency and roadmap

In the case of  $\text{CH}_3\text{NH}_3\text{PbI}_3$ , since the onset of light absorption is ca. 800 nm, the ideal maximum photocurrent is  $\sim 27 \text{ mA cm}^{-2}$  [47]. Provided 90% of IPCE is achievable between 400 nm and 800 nm,  $24 \text{ mA cm}^{-2}$  of photocurrent can be collected. Thin devices (200–300 nm of absorber) obtain the champion efficiencies, but the EQE slightly drops at wavelengths higher than 550 nm [1], indicating a lack of absorption in this range. Therefore, the incorporation of plasmonic absorbers could yield current enhancement due to better light harvesting [67–69] at low film thicknesses. Concurrently, a suppression of the recombination could lead to  $V_{\text{OCs}}$  of around 1.1 V (see Fig. 5a) in the ssDSC configuration with  $\text{TiO}_2$  and spiro-OMeTAD, and even higher in the thin film configuration. Under these considerations, efficiencies  $\sim 20\%$  becomes achievable with a FF of 75% (Fig. 5a), surpassing efficiencies of amorphous Si cells and bringing them to comparable levels of multicrystalline Si.

Thus far, much of the efforts have focused on  $\text{CH}_3\text{NH}_3\text{PbI}_3$ , however, there are reports of other candidates from this family of materials that are suitable for solar cells. Perovskite is a flexible structure type and many elements in the periodic table (such as  $\text{Co}^{2+}$ ,  $\text{Fe}^{2+}$ ,  $\text{Mn}^{2+}$ ,  $\text{Pd}^{2+}$ , and  $\text{Ge}^{2+}$ ) can be incorporated through various structural adaptations. The Goldschmidt tolerance factor [28,70] can be used for guidance as to which combinations of elements may form a stable structure. There is a drive to replace  $\text{Pb}^{2+}$  with a less toxic element with Sn as one of the obvious candidates. Nevertheless its easy oxidation creates  $\text{Sn}^{4+}$  that originates a metal-like behaviour in the semiconductor which lowers the photovoltaic performance [61]. Other alternatives that could be explored include other organic cations such as formamidinium. By introducing longer chained organic components at the 'A' site, perovskite-type layer compounds comparable to the Ruddlesden-Popper series [71] can be created. Ab-initio calculations [36] are therefore needed as guidance to identify newer families of photovoltaic perovskites.

Commercial viability of new energy generating technologies such as perovskite solar cells ultimately relies also on improved costs per Watt peak (Wp) of installation compared to existing competition in the marketplace (see Fig. 5b). With light-absorbers and electrode materials amenable to application techniques at low temperatures such as spray, blade coating and roll-to-roll printing, perovskite solar cells are promising high efficiency, lightweight, cost-effective options. The energy payback times for these solar cells, estimated to be similar to that of DSC's (i.e. less than one year compared with up to three years for silicon solar cells [2]) are an extra advantage over the competition. In a first step towards this

direction, completely low temperature processed ( $<90^\circ\text{C}$ ) solar cells with efficiencies close to 10% have been realized [72].

While estimating lifetime costs, one also needs to account for stability and toxicity in addition to high efficiencies. In the lab, 500 h device stabilities have already been reported in dry ambient [1,12], however it has also been reported that humidity degrades the  $\text{CH}_3\text{NH}_3\text{PbI}_3$  performance [37]. Halide alteration has been promising in this regard with increased stability in humid environments at minor performance penalty [37] occurring when a low proportion of Br (20% versus 80% I) is introduced. Lead content is another drawback for the viability of these cells. Although material restriction laws such as the European Union Restriction on Hazardous Substances (RoHS) can make exceptions for specific products (e.g. Cd in solar panels),  $\text{CH}_3\text{NH}_3\text{PbI}_3$  degradation under water exposure makes encapsulation studies vital for commercialization. The roadmap to successful commercialization thus entails the comprehensive understanding of the photovoltaic principles and degradation mechanisms, new materials development, optimization of device structure and related manufacturing technologies.

The rapid strides in the development of highly efficient organic/inorganic halide perovskite solar cells now demands attention to be paid to fundamental studies while simultaneously pursuing new materials and device development for the widespread deployment of this solution processed photovoltaic technology.

### Acknowledgements

The authors want to acknowledge the productive discussions with Thomas Baikie (NTU, Singapore), Damion Milliken and Hans Desilvestro (Dyesol Limited, Australia). This work was supported by the National Research Foundation Singapore (Project #: NRF-CRP4-2008-03) and SinBerISE CREATE programme.

### References

- [1] J. Burschka, et al. *Nature* 499 (2013) 316.
- [2] M. Graetzel, et al. *Nature* 488 (2012) 304.
- [3] B.C. O'Regan, M. Grätzel, *Nature* 353 (1991) 737.
- [4] A. Yella, et al. *Science* (New York, NY) 334 (6056) (2011) 629.
- [5] U. Bach, et al. *Nature* 395 (1998) 583.
- [6] J. Burschka, et al. *Journal of the American Chemical Society* 133 (2011) 18042.
- [7] I. Chung, et al. *Nature* 485 (2012) 486.
- [8] G. Hodes, D. Cahen, *Accounts of Chemical Research* 45 (2012) 705.
- [9] P. Maraghechi, et al. *ACS Nano* 7 (2013) 6111.
- [10] J.A. Chang, et al. *Nano Letters* 12 (2012) 1863.
- [11] M. Nanu, et al. *Nano Letters* 5 (2005) 1716.
- [12] H.-S. Kim, et al. *Scientific Reports* 2 (2012) 1.
- [13] M.M. Lee, et al. *Science* 338 (6107) (2012) 643.
- [14] J.H. Heo, et al. *Nature Photonics* 7 (2013) 486.
- [15] J.M. Ball, et al. *Energy & Environmental Science* 6 (2013) 1739.
- [16] N.-g. Park, *The Journal of Physical Chemistry Letters* 4 (2013) 2423.
- [17] C.K. Møller, *Nature* 180 (1957) 981.
- [18] C.K. Møller, *Nature* 182 (1958) 1436.
- [19] A. Kojima, et al. *Journal of the American Chemical Society* 131 (2009) 6050.
- [20] J.-H. Im, et al. *Nanoscale* 3 (2011) 4088.
- [21] J.H. Heo, et al. *The Journal of Physical Chemistry C* 116 (2012) 20717.
- [22] P. Mauersberger, F. Huber, *Acta Crystallographica Section B* 36 (3) (1980) 683.
- [23] K. Shum, et al. *Applied Physics Letters* 96 (22) (2010) 221903.
- [24] D.B. Mitzi, et al. *Inorganic Chemistry* 38 (26) (1999) 6246.
- [25] A. Kojima, et al. *Chemistry Letters* 41 (4) (2012) 397.
- [26] K. Tanaka, et al. *Solid State Communications* 127 (9/10) (2003) 619.
- [27] T. Ishihara, *Journal of Luminescence* 60–61 (1994) 269.
- [28] Z. Cheng, J. Lin, *CrystEngComm* 12 (2010) 2646.
- [29] H. Arend, et al. *Journal of Crystal Growth* 43 (2) (1978) 213.
- [30] T. Umebayashi, et al. *Physical Review B* 67 (15) (2003) 155405.
- [31] T. Baikie, et al. *Journal of Materials Chemistry A* 1 (18) (2013) 5628.

- [32] D.B. Mitzi, Synthesis, structure, and properties of organic–inorganic perovskites and related materials, in: *Progress in Inorganic Chemistry*, John Wiley & Sons, Inc., 2007. p. 1.
- [33] S. Zhang, et al. *Acta Materialia* 57 (2009) 3301.
- [34] K. Tanaka, et al. *Solid State Communications* 127 (2003) 619.
- [35] G.C. Papavassiliou, et al. *Advanced Materials for Optics and Electronics* 9 (6) (1999) 265.
- [36] E. Mosconi, et al. *The Journal of Physical Chemistry C* 117 (2013) 13902.
- [37] J.H. Noh, et al. *Nano Letters* 13 (2013) 1764.
- [38] H.-S. Kim, et al. *Nano Letters* 13 (2013) 2412.
- [39] K. Liang, et al. *Chemistry of Materials* 4756 (1998) 403.
- [40] P.K. Nayak, et al. *Energy & Environmental Science* 5 (2012) 6022.
- [41] D. Bi, et al. *RSC Advances* 3 (2013) 18762.
- [42] E. Edri, et al. *The Journal of Physical Chemistry Letters* 4 (2013) 897.
- [43] D. Bi, et al. *The Journal of Physical Chemistry Letters* 4 (2013) 1532.
- [44] L. Etgar, et al. *Journal of the American Chemical Society* 134 (42) (2012) 17396.
- [45] J.-y. Jeng, et al. *Advanced Materials* 25 (2013) 3727.
- [46] M. Liu, et al. *Nature* 501 (2013) 395.
- [47] H.J. Snaith, *Advanced Functional Materials* 20 (1) (2010) 13.
- [48] J. Qiu, et al. *Nanoscale* 5 (2013) 3245.
- [49] L. Etgar, et al. *Journal of the American Chemical Society* 134 (2012) 17396.
- [50] P.P. Boix, et al. *The Journal of Physical Chemistry C* 116 (2011) 1579.
- [51] P.P. Boix, et al. *ACS Nano* 6 (2012) 873.
- [52] G. Boschloo, A. Hagfeldt, *Chemical Physics Letters* 370 (2003) 381.
- [53] Q. Shen, et al. *Japanese Journal of Applied Physics* 45 (2006) 5569.
- [54] F. Fabregat-Santiago, et al. *Journal of the American Chemical Society* 131 (2009) 558.
- [55] M. Wang, et al. *Nature Chemistry* 2 (2010) 385.
- [56] M.M. Lee, et al. *Science (New York, NY)* 643 (2012) 1.
- [57] a.V. Shah, et al. *Progress in Photovoltaics: Research and Applications* 12 (23) (2004) 113.
- [58] G. Xing, et al. *Science* 342 (2013) 344.
- [59] G.E. Eperon, et al. *Advanced Functional Materials* 24 (2013) 151.
- [60] I. Chung, et al. *Journal of the American Chemical Society* 134 (2012) 8579.
- [61] C.C. Stoumpos, et al. *Inorganic Chemistry* 52 (2013) 9019.
- [62] N. Onoda-Yamamuro, et al. *Journal of Physics and Chemistry* 53 (1992) 935.
- [63] D. Mitzi, et al. *Nature* 369 (1994) 467.
- [64] D. Mitzi, et al. *Journal of Solid State* 114 (1995) 159.
- [65] D.B. Mitzi, et al. *Chemistry of Materials* 11 (1999) 542.
- [66] H.-s. Kim, et al. *Nature Communications* 4 (2013) 1.
- [67] H.A. Atwater, A. Polman, *Nature Materials* 9 (2010) 865.
- [68] B. Wu, et al. *Nature Communications* 4 (2013) 2004.
- [69] T.Z. Oo, et al. *The Journal of Physical Chemistry C* 116 (10) (2012) 6453.
- [70] V.M. Goldschmidt, IX (Oslo: Norske Vid., 1937), 1926.
- [71] B.V. Beznosikov, K.S. Aleksandrov, *Crystallography Reports* 45 (2000) 792.
- [72] H.K. Mulmudi, et al. *Chemical Communications* (2013).